Published by :
http://www.ijert.org

International Journal of Engineering Research & Technology (IJERT)
ISSN: 2278-0181
Vol. 5 Issue 05, May-2016

Conversion of Micro-Sized Zn Powder into Zno Nanoparticles and Nanopencils using Nanosecond Laser in Liquid

Q. A. Drmosh[1*],
[1] Laser Research Group,
Physics Department,and Center of Excellence in Nanotechnology (CENT),
King Fahd University of Petroleum & Minerals,
Dhahran 31261, Saudi Arabia

M. A. Gondal[2],
[2]Laser Research Group,
Physics Department, and Center of Excellence in Nanotechnology (CENT),
King Fahd University of Petroleum & Minerals,
Dhahran 31261, Saudi Arabia

T. F. Qahtan[3],
[3]Laser Research Group, and Physics Department,
King Fahd University of Petroleum & Minerals,
Dhahran 31261, Saudi Arabia

A. H. Y. Hendi[4]
[4]Physics Department,
King Fahd University of Petroleum & Minerals,
Dhahran 31261, Saudi Arabia

***Abstract* - Numerous techniques are being developed and investigated for the synthesis of high purity nanostructured semiconducting metal oxides due to their unique properties and vast applications in different fields. Among different metal oxide nanostructures, Zinc oxide (ZnO) nanostructures are promising candidate for various applications. In the present study, high purity ZnO nanoparticles and nanopencils were synthesized via nanosecond pulsed laser ablation of microstructured zinc (Zn) powder in deionized water (DIW). Structural, morphological, compositional, and optical properties of the synthesized ZnO nanostructures were characterized by means of X-ray diffraction (XRD), field emission scanning electron spectroscopy (FE-SEM), transmission electron microscopy (TEM), X-ray photoelectron spectroscopy (XPS), UV-Vis absorption, and photoluminescence (PL) techniques. The XRD analysis confirmed the crystalline structure of the synthesized ZnO while the XPS analysis revealed the formation of high purity ZnO. The FESEM and TEM images demonstrated the conversion of the spherical structure of the micro-sized Zn into nanoparticles and nanopencils ZnO. Our nano ZnO synthesized band gap was found to be blue shifted as compared to the bulk ZnO. The room temperature PL spectrum of the prepared ZnO nanostructures showed a single UV luminescence emission peak centered at 472 nm which is ascribed to direct band-to-band transition.**

Key Words: Pulsed laser ablation, nanoparticles and nanopencils, Photoluminescence

1. INTRODUCTION

Owing to the present and potential applications of metal oxide nanomaterials in the industry and medicine, researchers are looking for low cost and high production yield method to synthesize high purity nanomaterials. The growing increase in fabrication of nanostructured materials is ascribed to the superiority of their properties over those of bulk materials. These properties include their nano-scaled particle sizes and large surface area which play a major role in the enhancement of the chemical reactivity as compared to the corresponding bulk materials. Generally speaking, nanomaterials could be synthesized using two approaches: top-down and bottom-up. In top-down approach, nanomaterials can be fabricated by etching smaller particles from larger ones using various methods such as electro exploding wire, laser ablation and ball milling. However, bottom-up approach refers to the build-up of a material from the bottom: atom-by-atom, molecule-by-molecule, or cluster-by-cluster. Sol-gel and crystal growth are examples of bottom-up approach where growth species, atoms, ions or molecules, are orderly assembled into desired crystal structure [1].

ZnO, a wide band gap semiconductor (Eg = 3.31 eV), has received much interest in many applications such as catalyst [2-4], gas sensor [5], piezoelectric devices [6] and varistor [7]. Such wide applications are based on its high chemical stability and excellent optical and electrical properties which have shown size and shape dependence. Different synthesis methods based on physical and chemical techniques have been reported for preparation of nanosized ZnO including, sol–gel method [8], precipitation in alcoholic medium [9], Polyol synthesis [10], microemulsion [11], ball mailing [12], microwave assisted method [13], and hydrothermal route [14]

However, these synthesis methods require large amount of chemicals and involves rigorous experimental procedures as well as sophisticated equipment. Pulsed laser ablation in liquid (PLAL) has been widely used for fabrication of nanostructured ZnO by irradiating solid Zn target in different liquids [15]. In addition to its simplicity, such a technique has proved its efficiency in fabrication of high purity ZnO nanostructures [16]. Furthermore, this method requires the minimum amount of chemicals for synthesis nanostructured ZnO compared to the other chemical routes as well as tailoring the size and shape of the prepared nanostructed ZnO by suitable adjustment of laser parameters and liquid medium [17,18]. Nevertheless, this efficient method is suffered with low production yield since the laser beam is focused merely on small targeted area of Zn metal.

In the present study, high purity nanostructured ZnO with high production yield compared with PLAL of solid target were prepared by ablation of micro-sized Zn powder in DIW. The structural, morphological, compositional and optical properties of the prepared ZnO nanostructures were then characterized using various analytical techniques.

International Journal of Engineering Research & Technology (IJERT)
ISSN: 2278-0181
Vol. 5 Issue 05, May-2016

2. EXPERIMENTAL

ZnO nanostructures were synthesized by PLAL of Zn powder in DIW at room temperature. A high purity Zn powder (99.998 %, Aldrich) was mixed in 10 ml of DIW and the solution was then kept under high speed magnetic stirring for 20 min to obtain a homogeneous mixture. The ablation was carried out with A Q-switched Nd-YAG laser (Spectra physics Model GCR 100) operating with a pulse width of 8 ns and operates at a 10 Hz pulse repetition rate. Ablation was achieved with laser operating at 355 nm wavelength using third harmonic generator of maximum pulse energy of 300 mJ as an excitation source. The schematic set-up was presented in Fig. 1. The beam of laser was focused onto the middle of the cell containing the mixture for 120 minutes to obtain a white colloidal solution based on ZnO.

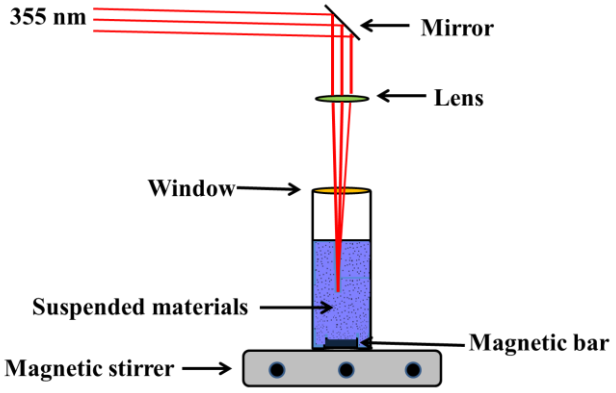

Fig -1: Typical set up for pulsed laser ablation of micr-sized particles in liquid media

3- INSTRUMENTATION

A variety of analytical techniques were applied for the characterization of the raw Zn powder and nanostructured ZnO prepared by PLAL in DIW. The crystal structure and the average crystal size were characterized via XRD (Shimadzu XRD 6000), with Cu Kα irradiation at λ = 1.5418 Å and 2θ scanning rate of 2°/min. The morphology of samples was investigated using FE-SEM (Tescan Model Lyra3) with an operating voltage of 20 kV and TEM (FEI Tecnai G2 20 S-TWIN.). Chemical analysis was performed using X-ray photoelectron spectroscopy (XPS, ESCALAB 250Xi, Thermo Scientific) equipped with a monochromatic Al Ka (1486.6eV) X-ray source. Binding energies for all high-resolution spectra were calibrated using C 1s at 284.6 eV as a charge reference. Prior to XPS analysis, sample was transferred in air to the XPS chamber and the analyzing chamber was evacuated to a base pressure of 7×10-9 mbar. UV−vis absorbance spectra were measured by a JASCO UV-V-570 spectrophotometer. The Photoluminescence (PL) measurements of synthesized ZnO nanostructures were carried out using a spectrofluorometer (Horiba Model FluoroLog-3) equipped with 150W Xe lamp as an excitation source.

4- RESULTS AND DISCUSSION

4.1 Structural And Compositional Analysis

Paragraph comes content here To study the structural properties of the raw Zn powder and nanostructured ZnO prepared by PLAL of Zn powder in DIW, a systematic analysis of their XRD patterns was carried out in the 2θ range of 10°-80°. Typical XRD patterns of the micro-sized Zn powder are displayed in Fig. 2a. All diffraction peaks are assigned to the hexagonal structure phase of Zn. Fig. 2b shows typical XRD spectrum of nanostructured ZnO. The main dominant peaks for ZnO nanostructures were identified at 2θ = 31.52°, 34.18°, 36.06°, 47.30°, 56.30°, 62.62°, 65.92°, 67.74°, 68.74° and 76.68° corresponding to (100), (002), (101), (102), (110), (103), (220), (112), (201) and (202) planes. The crystalline size (D) of the prepared ZnO nanostructures was estimated using the Debye Scherrer equation:

$$D = \frac{0.9\lambda}{\beta \cos\theta}$$

where, λ is the X-ray wavelength, β is the full width at half maximum (FWHM), and θ is the diffraction angle

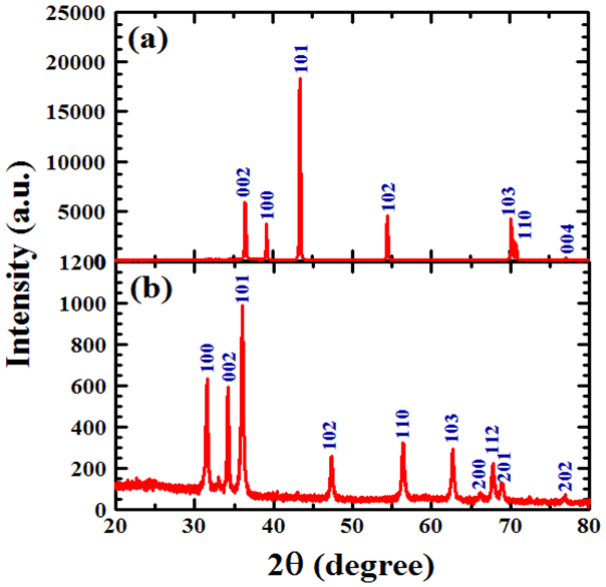

Fig -2: XRD patterns of a) micro-sized Zn and b) nano-sized ZnO prepared by PLAL method.

The average crystal size of the synthesized ZnO nanostructures calculated from the most intense peak is about 34 nm. The lattice parameters a and c of the synthesized ZnO nanostructures were estimated from the formula of the hexagonal structure [19]:

$$1/d^2 = (4/3\, a^2)(h^2 + hk + k^2) + l^2/c^2$$

where h, k, and l are miller indices of the reflecting planes and d is the inter planar spacing.

The most intense peaks correspond to the (100) and (002) planes were used to determine the values of (a and c) of the prepared ZnO nanostructures which were found to be 0.3291 nm and 0.5273 nm, respectively. These values are slightly greater than the typical values of the corresponding lattice parameters of the bulk ZnO (a = 0.3249 nm, c = 0.5205 nm), which may be attributed to the lattice expansion in nano-scale [20-22]. The surface chemical analysis of the prepared ZnO nanostructures was carried out using XPS. A typical XPS spectrum for the survey of the prepared ZnO nanostructures in the binding energy range 0-1300 eV is

International Journal of Engineering Research & Technology (IJERT)
ISSN: 2278-0181
Vol. 5 Issue 05, May-2016

shown in Fig. 3 (a), which reveals the presence of the main constituents (Zn and O). The O1s spectrum in the energy range 525-535 eV (Fig. 3 (b)) showed a broad peak centered at binding energy of 530 eV and the fitting of this peak shows two Gaussian peaks at 529.52 eV and 531.18 eV. The peak centered at binding energy of 529.52 eV is attributed to $O2^-$ ions in the ZnO lattice [23] while the peak centered at binding energy of 531.18 eV is assigned to OH dissociation on the surface of the sample [24]. The Zn 2p region in the binding energy range 1010-1060 eV (Fig. 3(c)) contains two core peaks centered at 1021.29 eV and 1044.18 eV which are ascribed to the spin-orbit split doublet of Zn 2p3/2 and Zn 2p1/2, respectively [25]. The electron binding energy difference (δ) between the two core peaks is 22.89 eV which is in a good agreement with 23.0 eV [26].

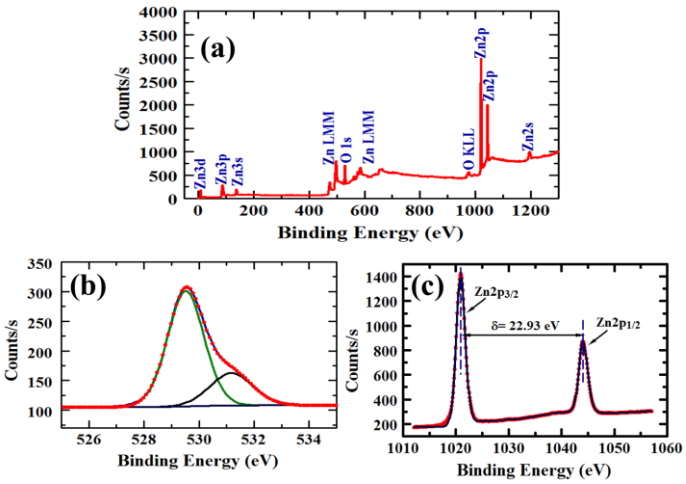

Fig -3: Wide scan XPS spectrum and (b-c) O 1s, and Zn 2p core level XPS spectra of the nanostructures ZnO prepared by PLAL method

4.2 Morphology

The morphological properties of the raw Zn powder and ZnO nanostructures prepared by PLAL technique were characterized by FESEM and TEM techniques. Figures 4(a) and 4(b) show the low and high magnification FESEM images of micro-sized Zn. It can be observed that Zn particles are spherical in shape with a diameter ranging between 1- 4 µm. Figures 4(c) and 4(d) display the TEM images of the synthesized nanostructured ZnO. As can be noticed, the spherical structure of the micro-sized Zn has been converted into ZnO nanoparticles and nanopencils. The diameter of the fabricated ZnO nanoparticles ranges from 10–25 nm whereas the length of the nanopensils varying between 23 and 60 nm. It can also be observed that the particle size observed in TEM measurement is different than the average crystal size measured by XRD technique which could be attributed to the formation of ZnO nanostructures in different shapes (nanoparticles and nanopencils).

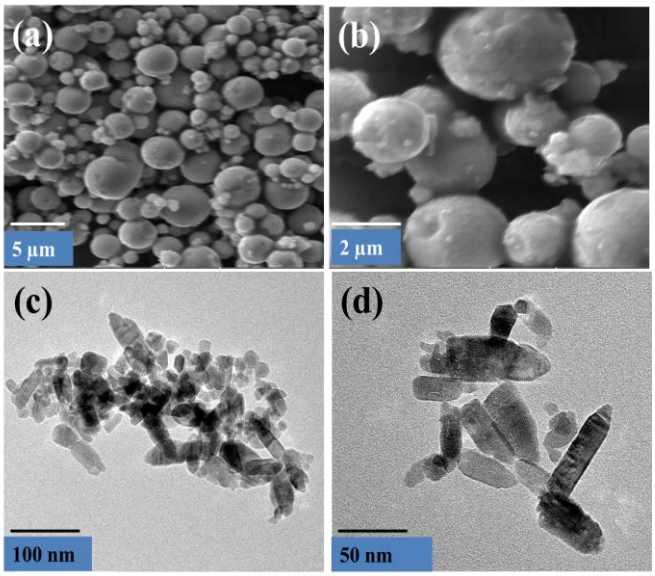

Fig -4: (a and b) FE-SEM micrographs of the micro Zn particles and (c and d) TEM images of the synthesized ZnO nanostructures

1.1 Optical Absorption

Fig.5 shows UV-visible spectrum of colloidal solution obtained by PLAL technique. As can be seen, the ZnO absorption peak was observed at 343 nm which shows a significant blue shift corresponding to bulk absorption peak centered at (360 nm) [27]. This blue shift may originate from the quantum confinement of nanostructures.

The optical bandgap (E_g) was estimated from the optical absorption coefficient (α) using the following formula:

$$\alpha E = A(h\nu - E_g)^{1/2}$$

where, E is the photon energy, E_g is the direct band gap of the semiconductor, A is a constant. Therefore, a plot of $(\alpha E)^2$ versus photon energy E should yield a straight line that intercepts the photon energy axis at the band gap. The calculated band gap (inset of fig. 5) was found to be 3.39 eV showing a slight increase compared to the band gap of the bulk ZnO.

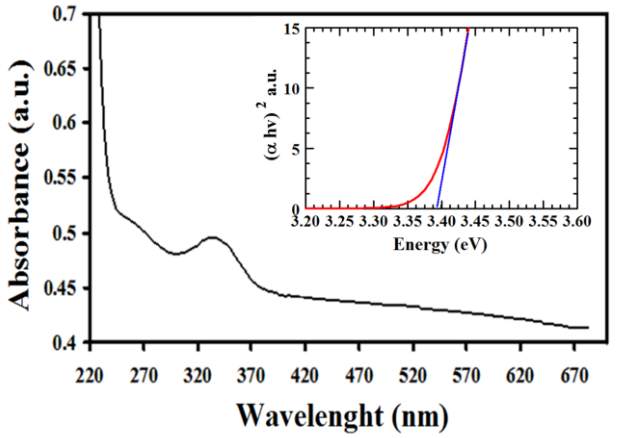

Fig -5: UV absorption spectrum of ZnO nanostructuress synthesized by PLAL technique

International Journal of Engineering Research & Technology (IJERT)
ISSN: 2278-0181
Vol. 5 Issue 05, May-2016

This increase in the band gap of ZnO could be attributed to the reduction in the crystalline size which can be ascribed by Brus formula [28-29].

$$E_g = E_g^{bulck} + \frac{\hbar^2 \pi^2}{2r^2}\left(\frac{1}{m_e} + \frac{1}{m_h}\right) - \frac{1.8}{4\pi\varepsilon\varepsilon_0 r} e^2$$

where E_g^{bulk} is the bulk energy bandgap, r is the particle radius, $\hbar$ is Planck's constant ivied by 2π, m_e is the effective mass of the electrons, m_h is the hole effective mass, ε is the relative permittivity, ε_0 is the permittivity of vacuum, and e is the charge of the electron.

4.4 Photoluminescence

Study of the photoluminescence (PL) property of the prepared ZnO nanostructures is interesting because it can offer valuable information on their quality and purity. Fig.6 depicts the room temperature PL spectrum of ZnO nanostructures prepared by PLAL in DIW. The PL measurement of the fabricated sample was performed at an excitation wavelength of 320 nm and the PL emission was measured in the wavelength ranging from 350-600 nm. The excitation wavelength was selected from photoluminescence excitation of the prepared ZnO nanostructures which shows an intense peak at 320 nm. Under this excitation wavelength, an intense and sharp UV emission peak centered at 372 nm was observed. In general, the photoluminescence of ZnO nanostructures can be divided into two photoluminescence bands: (1) UV emission band typically in the range of 350 to 400 nm and (2) visible emission band ranging from 400 to 600 nm. The UV emission peak is explained due to the recombination of electron hole in semiconductors [30-31] while the PL emission in the visible region resulted from structure defects such as zinc vacancy, zinc interstitial, oxygen vacancy, oxygen interstitial, antisite oxygen [32-34].

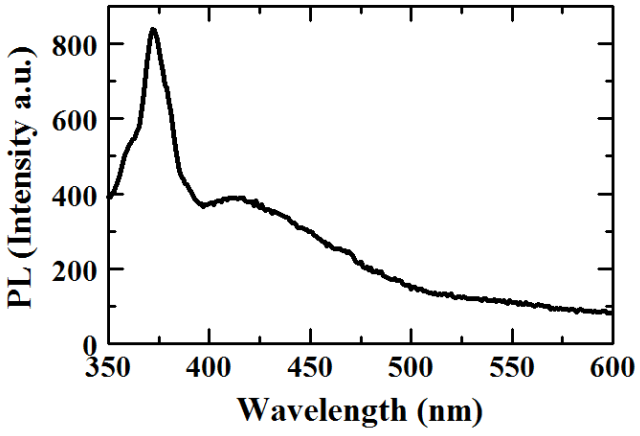

Fig -6: Room-temperature photoluminescence spectrum of the ZnO nanoparticles prepared by PLAL technique in DIW (at excitation 320nm).

5. CONCLUSIONS

In this work, high purity nanostructured ZnO with high production yield was fabricated via nanosecond laser ablation of micro-sized Zn particles in DIW. The prepared ZnO nanostructures were then characterized using various analytical techniques. The XRD pattern confirmed the crystalline structure of the synthesized ZnO while the XPS analysis revealed the formation of high purity ZnO. The FESEM and TEM images presented the conversion of the spherical structure of the micro-sized Zn into nanoparticles and nanopencils ZnO. The optical band gap was found to be blue shifted as compared to the bulk ZnO. The PL spectrum of the prepared ZnO nanostructures exhibited sharp UV band corresponding to band gap excitonic emission.

ACKNOWLEDGEMENT

The support by the Physics Departments and Center of Excellence in Nanotechnology (CENT) and King Fahd University of Petroleum and Minerals under project # Rg 1311 is gratefully acknowledged.

REFERENCES

[1] S. Verma, R. Gokhale, J. Burgess, International Journal of Pharmaceutics. 380, 216 (2009).
[2] C. Hariharan, Revisited Applied Catalysis A: General. 304, 55 (2006).
[3] H. Wang, C. Xie, W. Zhang, S. Cai, Z. Yang, Y. Gui, Journal of Hazardous Materials. 141, 645 (2007).
[4] A. Akyol, M. Bayramo˘glu, Journal of Hazardous Materials B. 124, 241 (2005).
[5] H. Yoo,H. Kim, D. Kim.Nanoscience an Nanotechnology Letters. 7, 758 (2015).
[6] M.K. Gupta, N. Sinha, B.K. Singh, N. Singh, K. Kumar, Binay Kumar, Materials Letters. 63, 1910 (2009).
[7] H. Xu, X. Liu, D. Cui, M. Li, M. Jiang, Sensors and Actuators B: Chemical. 114, 301 (2006).
[8] Y. Liu, Q. W. Kou, S. Xing, C. Y. Mao, N. Kadasala, Q. Han, J. L. Song, H. L. Liu, Y. Q. Liu, Y. S. Yan, and J. H. Yang. Nanosci. Nanotechnol. Lett. 7, 665 (2015).
[9] L. Spanhel, M.A. Anderson, Journal of American Chemistry Society. 113, 1991 (1991).
[10] A. Dakhlaoui, M. Jendoubi , L. S. Smiri , A. Kanaev, N. Jouini, Journal of Crystal Growth. 311, 3989 (2009).
[11] J. C. Lin, C.P. Leeb and K. C. Ho. J. Mater. Chem. 22, 1270 (2012).
[12] S. Amirkhanlou, M. Ketabchi, N. Parvin. Materials Letters. 86, 122 (2012).
[13] V. Kumar, M. Gohain, S. Som, V. Kumar, B. Bezuindenhoudt, Physica B 480, 36 (2016).
[14] G. Patrinoiu, J. C. Moreno, C. M. Chifiriuc, C. Saviuc, R. Birjega, O. Carp. Journal of Colloid and Interface Science 462, 64 (2016).
[15] M.A. Gondal, Q.A. Drmosh, Z.H. Yamani, M. Rashid, International Journal of Nanoparticles. 2, 119 (2009).
[16] M.A. Gondal, Q.A. Drmosh, Z.H. Yamani, T.A. Saleh. Applied Surface Science. 256, 298 (2009).
[17] G. G. Guillen, M. I. Palma, B. Krishnan, D. Avellaneda, G. A. Castillo, T. K. Das Roy, S. Shaji. Materials Chemistry and Physics.162, 561 (2015).
[18] R.K. Thareja, S. Shukla, Applied Surface Science. 253, 8889 (2007).
[19] C. Suryanarayana, M.G. Norton, Plenum Press, New York, (1998).
[20] Ü. Özgür, Y. I. Alivov, C. Liu, A. Teke, M. Reshchikov, S. Doğan, V. Avrutin, S. Cho, and H. Morkoç, Journal of Applied Phyics. 98, 041301 (2010).
[21] Z. Wei, T. Xia, J. Ma, W. Feng, J. Dai, Q. Wang, P. Yan, Materials Characterization. 58, 1019 (2007).
[22] M. Fukuhara, Physics Letters A. 313, 427 (2003).
[23] S. K. Marathe, P. M. Koinkar, S. S. Ashtaputre, M. A. More, S. W. Gosavi, D. S. Joag and S. K. Kulkarni, Nanotechnology. 17, 1932 (2006).
[24] P.T. Hsieh, Y.C. Chen1, K.S. Kao, C.M. Wang, Appl. Phys. A. 90, 317 (2008).
[25] S. Karamat, C. Ke, T.L. Tan, W. Zhou, P. Lee, R.S. Rawat, Appli. Sur. Sci. 255, 4814 (2009).

International Journal of Engineering Research & Technology (IJERT)
ISSN: 2278-0181
Vol. 5 Issue 05, May-2016

[26] R. Al-Gaashani, S. Radiman, A. R. Daud, N. Tabet, Y. Al-Douri, , Ceramics International. 39, 2283 (2013).
[27] L. Shi, X. Li. Journal of Luminescence. 131, 834 (2011).
[28] L.E. Brus, J. Chem. Phys. 80, 4403 (1984).
[29] K. Lin, Hsin-Ming Cheng, Hsu-Cheng Hsu, Li-Jiaun Lin,Wen-Feng Hsieh, Chemical Physics Letters. 409, 208 (2005).
[30] M. Anpo and Y. Kubokawa, J. Phys. Chem. 88, 5556 (1984).
[31] A. van Dijken, E. A. Meulenkamp, D. Vanmaekelbergh, and A. Meijerink, J. Lumin. 87, 454 (2000).
[32] K. Vanheusden, W.L. Warren, C.H. Seager, D.R. Tallant, J.A. Voigt, B.E. Gnade, Journal of Applied Physics. 79, 7983 (1996).
[33] X. Wu, G. G. Siu, C. L. Fu, H. C. Ong, Applied Physics Letter. 78, 2285 (2001).
[34] N. E. Hsu, W. K. Hung, and Y. F. Chen, J. Appl. Phys. 96, 4671 (2004).

BIOGRAPHIES

Q.A. Drmosh received his PhD degree in Physics from King Fahd University of Petroleum and Minerals, Saudi Arabia, in 2015. Area of expertise: thin films, chemical sensors, laser ablation.

M. A. Gondal received his PhD from University, Bonn, Germany, 1983. He is currently distinguished Professor, and Coordinator of Laser Research Group at King Fahd University of Petroleum and Minerals, Saudi Arabia.

T. F. Qahtan is a PhD student in the Physics Department at King Fahd University of Petroleum and Minerals, Saudi Arabia.

Abdulmajeed H. Hendi, is a Lecturer in the Physics Department at King Fahd University of Petroleum and Minerals. Besides, he is doing his PhD in the area of thin films and nanomaterials.